



# One-pot efficient Heck coupling in water catalyzed by palladium nanoparticles tethered into mesoporous organic polymer

John Mondal, Arindam Modak, Asim Bhaumik\*

Department of Materials Science, Indian Association for the Cultivation of Science, Jadavpur 700 032, India

## ARTICLE INFO

### Article history:

Received 6 July 2011

Received in revised form 7 September 2011

Accepted 10 September 2011

Available online 16 September 2011

### Keywords:

Carbon–carbon bond

Heck coupling

Heterogeneous catalyst

Palladium nanoparticles

Mesoporous polymer

Water as solvent

## ABSTRACT

A new palladium grafted mesoporous organic polymer catalyst has been synthesized through the reaction of palladium(II) acetate with mesoporous poly-triallylamine (MPTA-1) in methanol. Powder XRD, HR TEM, FE SEM-EDS, AAS, UV–vis spectroscopic tools are employed to characterize this supported palladium catalyst Pd–MPTA-1. The Heck coupling reactions between a series of aryl halides and alkenes have afforded the corresponding C–C coupling products in good yield over this Pd-catalyst using water as reaction medium. This protocol provides a simple strategy for the generation of a variety of new C–C bonds by using this recyclable heterogeneous catalyst under environmentally benign conditions.

© 2011 Elsevier B.V. All rights reserved.

## 1. Introduction

Palladium catalyzed coupling of aryl halides with olefins usually referred to as Heck coupling and this is a well-established methodology in modern organic synthesis for the designing new C–C bond in a target organic molecule [1–5]. The importance and versatility of this strategy for C–C bond formation is felt in a diverse array of research interests ranging from natural product [6] to bioactive compound syntheses [7–9] as well as to the development of organic electronics [10]. This C–C bond formation reaction has a wider application on industrial scale production of nonsteroidal anti-inflammatory drugs naproxen [11] and nimesulide [12] too. Heck arylation has wide-scale research interest over other cross-coupling reactions due to functional group tolerance, ready availability and low cost of simple olefins [13]. Palladium nanoparticle based heterogeneous catalysts supported on insoluble inorganic matrices have gained an increasing attention in the environment-friendly catalytic applications over the past decade [14–18]. Homogeneous palladium nanoparticle systems usually have higher catalytic activity compared to their heterogenized counterpart. However, successful heterogenization is essential since Pd has a tendency to leach out irreversibly from the support preventing recyclability of the catalyst. Heterogenization is usually achieved by immobilizing palladium nanoparticles

on insoluble solid support such as porous silica [19–22], alumina [23] and also polymers [24]. Very recently, the use of functionalized mesoporous materials grafted with active metal centers at their surfaces has attracted considerable attention due to their huge potential applications in different catalytic reactions [25–29]. High surface area and distribution of the active metal sites at the surface of the pores make these materials exceptionally useful to carry out organic transformations under liquid phase conditions.

In this context, mesoporous organic polymers carrying the organic functional groups at the surface of the mesopores [30–34] can provide an ideal tethering agent for the active metals to bind at its surface strongly. Due to extensive cross linking, polymeric materials are highly desirable material for long term stabilization of the entrapped metal centers, which reduces the possibility of leaching of the metal under reaction conditions [35]. On the other hand, Heck reactions are most frequently performed in dipolar aprotic organic solvents such as DMF, DMSO, CH<sub>3</sub>CN, N-methylpyrrolidone (NMP), THF, triethanolamine or dioxane [36–38]. Due to the hydrophobic nature of the mostly used homogeneous catalysts (metal complexes bearing organic ligands), use of water as a solvent is quite rare in those coupling reactions. Instead, the reactions have been conducted using ionic liquid [39] as the solvent and under high temperature conditions (*ca.* 200 °C) to overcome this problem associated with the interaction between the catalyst and solvent. In this context the prospects of Pd-grafted heterogeneous catalysts are very exciting as they can provide ease of product separation, recovery of catalyst by simple filtration and excellent recycling efficiency compared to their homogeneous counterparts. Though

\* Corresponding author. Tel.: +91 33 2473 4971; fax: +91 33 2473 2805.  
E-mail address: [msab@iacs.res.in](mailto:msab@iacs.res.in) (A. Bhaumik).

heterogeneous Pd-catalysts have been used for Heck reaction in different organic solvents, it would be environmentally acceptable if the reaction can be carried out in water. Today a considerable effort has been devoted to perform organic reactions in aqueous medium replacing the hazardous organic solvents, because of its environmental acceptability, abundance and low cost [40–42]. Catalytic reactions that can be carried out using water as solvent and having good catalyst separation and recycling efficiency are of immense importance as they can meet these growing demands of green chemistry.

Very recently we have reported the synthesis of a mesoporous poly-triallylamine (MPTA-1) using an anionic surfactant sodium dodecylsulfate as template [43]. Surface of this mesoporous polymer contains N-donor sites, which can tether with Pd strongly. Herein we report, the strategy for the synthesis of a new mesoporous poly-triallylamine supported Pd-NPs (Pd-MPTA-1) and its excellent catalytic activity in the Heck coupling reaction of aryl halides and olefins, where the reactions are carried out in aqueous medium.

## 2. Experimental

### 2.1. Preparation of the catalyst

Synthesis of mesoporous polymer MPTA-1 was carried out as described before [43]. To a well stirred solution of this mesoporous polymer (500 mg of extracted MPTA-1 suspended into 20 ml of methanol) 50 mg of palladium(II) acetate was added and the resulting mixture was refluxed for about 6 h under nitrogen atmosphere. The color of the mixture was slowly changed from light yellow to black and no further color change occurred on further reflux. Then the reaction mixture was cooled to room temperature, filtered and washed by methanol. The black colored material was dried in air. This Pd-loaded mesoporous polymer has been designated as Pd-MPTA-1 and used as a catalyst for the Heck coupling reactions.

### 2.2. General procedure for Heck coupling of aryl halide with styrene

In a typical reaction a solution of iodobenzene (204 mg, 1 mmol), styrene (156 mg, 1.5 mmol) in 4 ml of water, Pd-MPTA-1 (10 mg) and  $K_2CO_3$  (276 mg, 2 mmol) were added, and the mixture was refluxed at 100 °C in an oil bath under nitrogen atmosphere. The progress of the reaction was monitored with TLC. After completion of reaction, the mixture was allowed to cool at room temperature. The reaction mixture was diluted with  $Et_2O$  (20 ml) and was extracted with  $Et_2O$  with the addition of water (2 × 2 ml). The combined organic layer was washed with brine and dried over anhydrous  $Na_2SO_4$ . Then the organic phase was evaporated to dryness to leave the crude product as white colored solid *trans*-stilbene. The isolated crude product was characterized by  $^1H$  and  $^{13}C$  NMR. This procedure was followed for all the reactions of aryl iodide with styrene listed in Table 1. The same procedure was followed for aryl bromides and chlorides using  $Cs_2CO_3$  as a base instead of  $K_2CO_3$  and the results are listed in Tables 2 and 3, respectively.

### 2.3. General procedure for Heck coupling of aryl halide with acrylic acid

In a typical reaction 10 ml of round bottomed flask iodobenzene (204 mg, 1 mmol), acrylic acid (108 mg, 1.5 mmol),  $K_2CO_3$  (276 mg, 2 mmol), and Pd-MPTA-1 (10 mg) were mixed with the addition of 4 ml of water. The resulting mixture was refluxed under nitrogen atmosphere at 100 °C till completion (monitored through TLC). The reaction mixture was cooled down to room temperature and

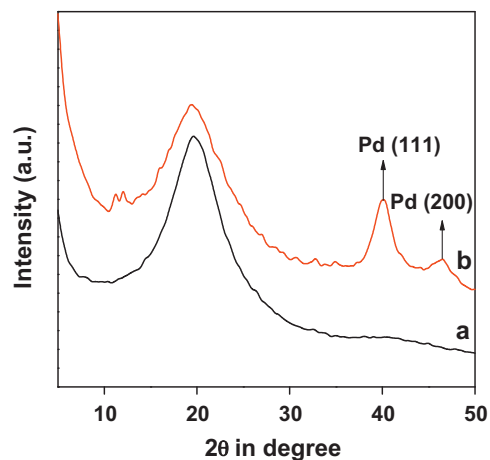


Fig. 1. Wide angle powder XRD pattern of the MPTA-1 (a) and Pd-MPTA-1 (b).

solid catalyst was separated by filtration. A white precipitate was appeared after acidification with concentrated sulfuric acid. Then the filtrate was extracted with ethyl acetate (20 ml) with the addition of water (2 × 2 ml). The combined organic layer was washed with brine and dried over anhydrous  $Na_2SO_4$ . The organic phase was evaporated to dryness to give the crude product *trans*-cinnamic acid as a white colored solid. The crude product was characterized by  $^1H$  and  $^{13}C$  NMR. The same procedure was followed for aryl bromides and chlorides using  $Cs_2CO_3$  as a base and the details are listed in Tables 2 and 3, respectively.

### 2.4. Recovery of the catalyst

After the reaction was over, reaction mixture was centrifuged and filtered. Then the catalyst was washed with water (5 × 3 ml) followed by  $Et_2O$  (3 × 4 ml). Then the catalyst was dried at 75 °C for 6 h for further use. Then the catalyst was recycled for three times for the coupling reaction between iodobenzene and styrene without loss of activity.

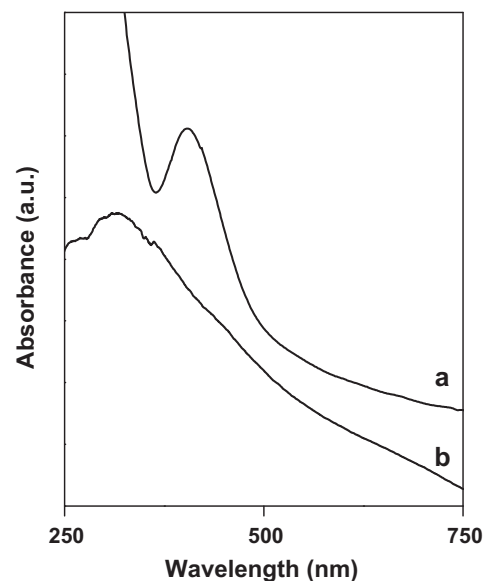


Fig. 2. UV-vis spectrum of the  $Pd(OAc)_2$  in chloroform (a) and diffuse reflectance spectrum of Pd-MPTA-1 in solid state (b).

Table 1

$$\text{Ar-I} + \text{R}-\text{CH}=\text{CH}_2 \xrightarrow{\text{Pd-MPTA-1, K}_2\text{CO}_3, \text{H}_2\text{O, Reflux}} \text{Ar}-\text{CH}=\text{CH}-\text{R}$$

Pd-MPTA-1 catalyzed C–C cross-coupling of aryl iodides<sup>a</sup>

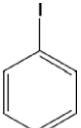
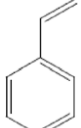
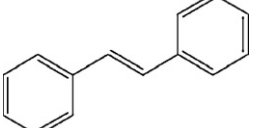
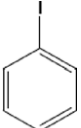
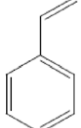
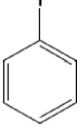
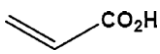
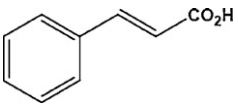
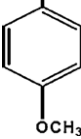
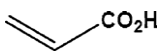
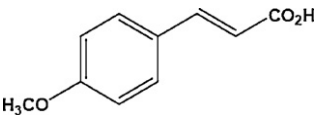
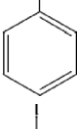
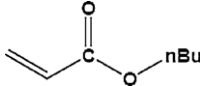
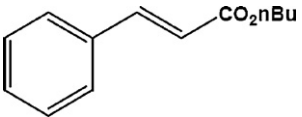
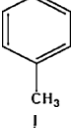
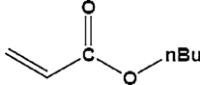
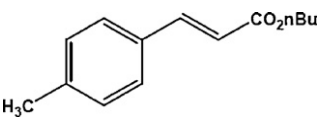
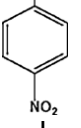
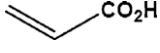
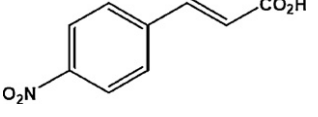
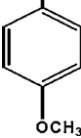
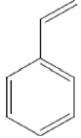
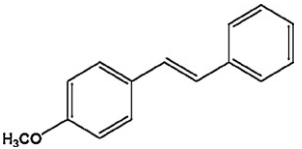
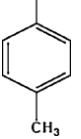
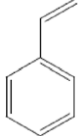
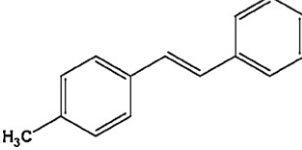
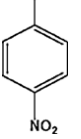
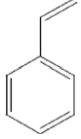
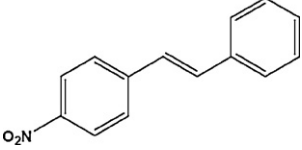
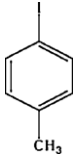

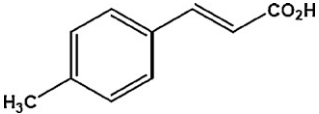
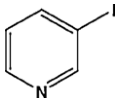
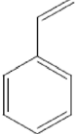
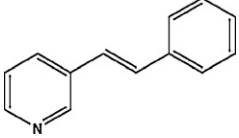
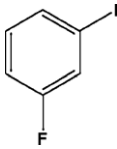
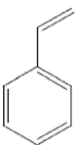
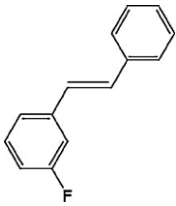
Entry	Aromatic bromides <sup>a</sup>	Aromatic alkenes	Time (h)	Yield (%) <sup>b</sup>	Products	TOF (h <sup>-1</sup> ) <sup>c</sup>
1			6	92		217
2 <sup>d</sup>			8	–	–	–
3			4	94		332
4			5	93		263
5			5	93		263
6			4	95		336
7			6	89		210
8			5	90		255
9			5	92		260
10			4	88		182

Table 1 (Continued)

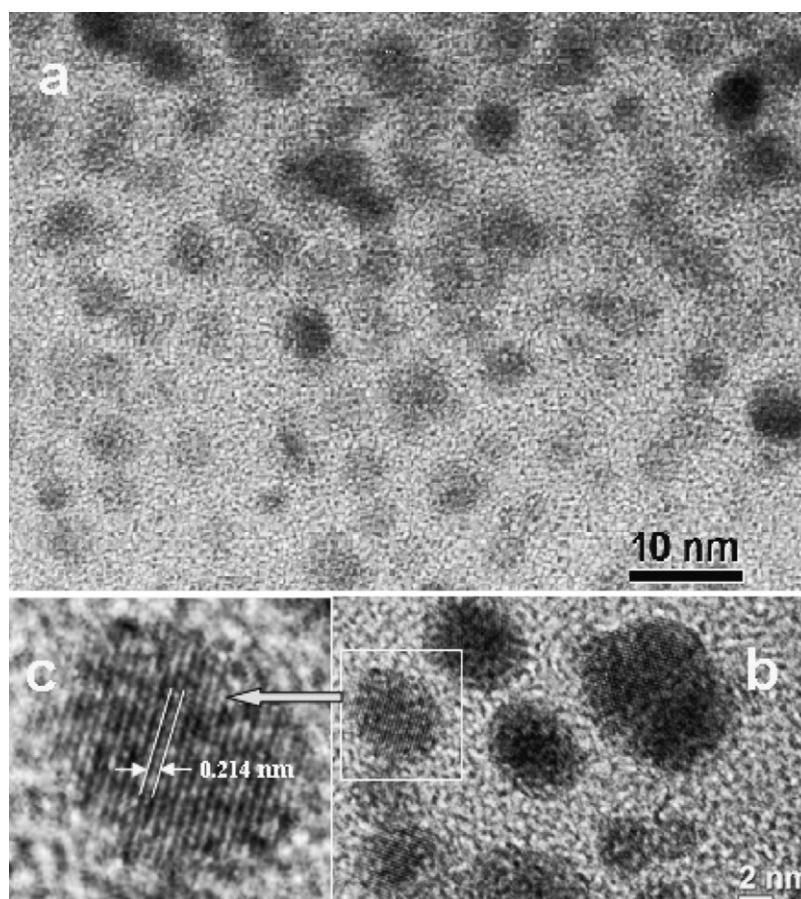
Entry	Aromatic bromides <sup>a</sup>	Aromatic alkenes	Time (h)	Yield (%) <sup>b</sup>	Products	TOF (h <sup>-1</sup> ) <sup>c</sup>
11			7	90		182
12			6	92		217
13			7	90		182

<sup>a</sup> Reaction conditions: Ar-I (1.0 equiv.), alkene (1.5 equiv.), K<sub>2</sub>CO<sub>3</sub> (2 equiv.), water (4 ml), reaction temp. 100 °C, catalyst (10 mg).

<sup>b</sup> Isolated yield of pure product.

<sup>c</sup> Turn over frequency (TOF) = moles of substrate converted per mole of Pd per h.

<sup>d</sup> Reaction was carried out at 298 K.

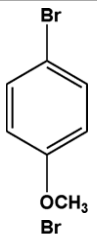
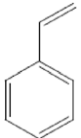
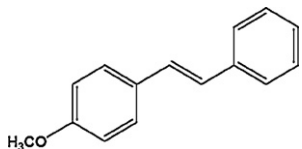
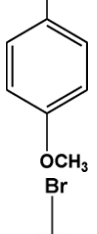
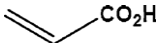
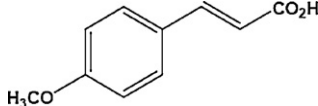
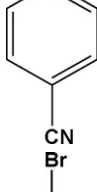
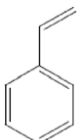
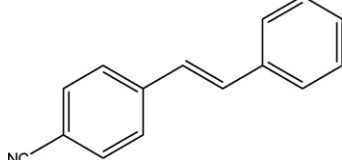
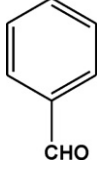
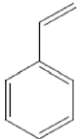
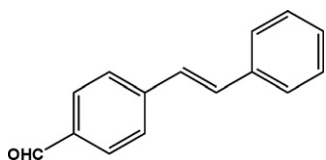
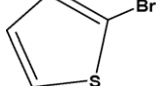
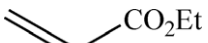
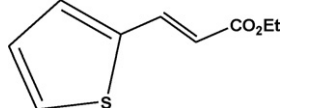


**Fig. 3.** TEM image of the Pd-MPTA-1 (a). HR TEM image of Pd-MPTA-1 (b) and crystalline palladium nanoparticles with resolvable atomic lattice (c).

Table 2

$\text{Ar-Br} + \text{R-CH=CH}_2 \xrightarrow{\text{Pd-MPTA-1, Cs}_2\text{CO}_3, \text{H}_2\text{O, Reflux}} \text{Ar-CH=CH-R}$

Pd-MPTA catalyzed C–C cross-coupling of aryl bromides<sup>a</sup>

Entry	Aromatic bromides <sup>a</sup>	Aromatic alkenes	Time (h)	Yield (%) <sup>b</sup>	Products	TOF (h <sup>-1</sup> ) <sup>c</sup>
1			4	90		318
2			5	88		249
3			5	92		260
4			6	88		208
5			4	90		318

<sup>a</sup> Reaction conditions: Ar–Br (1.0 equiv.), alkene (1.5 equiv.), Cs<sub>2</sub>CO<sub>3</sub> (2 equiv.), water (4 ml), 100 °C, catalyst (10 mg).

<sup>b</sup> Isolated yield of pure product.

<sup>c</sup> Turn over frequency (TOF) = moles of substrate converted per mole of Pd per h.

### 2.5. Sample preparation for the estimation of Pd

Palladium loading in the Pd–MPTA-1 catalyst was determined through AAS analysis. In order to measure palladium loading in the Pd–MPTA-1 at first three standard solutions with different concentrations Pd, 1 ppm, 2 ppm and 4 ppm have been prepared by dissolving required amount of Pd(OAc)<sub>2</sub> in water. Then 0.040 g Pd loaded catalyst Pd–MPTA-1 was dissolved into 5 ml 5 wt% of HNO<sub>3</sub> and it was digested. Then the resulting solution was diluted into a 25 ml volumetric flask by adding distilled water. This stock solution was used for the chemical analysis of Pd.

## 3. Results and discussion

### 3.1. Characterizations

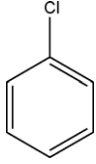
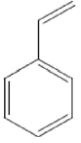
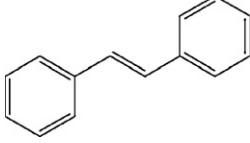
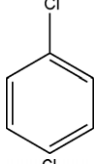
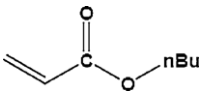
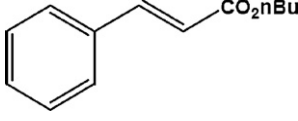
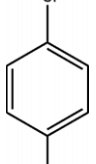
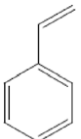
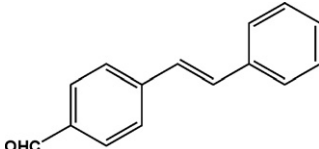
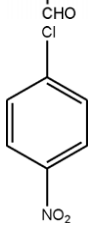
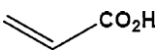
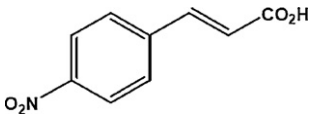
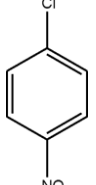
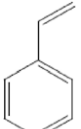
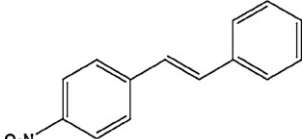
The catalyst was prepared by refluxing the mesoporous polymer MPTA-1 with palladium(II) acetate in methanol solvent. Methanol

acts as solvent and reducing agent to reduce Pd(II) to Pd(0), which can be capped at the surface of the mesoporous polymer MPTA-1. The formation of palladium nanoparticles was confirmed from the wide angle powder XRD pattern of Pd–MPTA-1 (Fig. 1). The figure shows two characteristic diffractions at 2θ value of 40.10 and 46.47, which are attributed to the presence of (111) and (200) planes of Pd(0), respectively. This result indicates that the palladium nanoparticles forms face centered cubic structure at the surface of Pd–MPTA-1. Another prominent peak at the 2θ value of 19.61 of the mesoporous polymer indicates that the presence of the mesoporous polymer matrix of MPTA-1 in the catalyst [43]. The BET surface areas of the template-free MPTA-1 and Pd–MPTA-1 are 134 m<sup>2</sup> g<sup>-1</sup> [43] and 12 m<sup>2</sup> g<sup>-1</sup>, respectively. A considerable decrease in the BET surface area of Pd–MPTA-1 material suggests that considerable amount of Pd centers have been anchored on the inner surface of the pores. UV–vis spectrum of the Pd(OAc)<sub>2</sub> shows the absorption band with the maximum at 400 nm (Fig. 2), which is referred to the existence of Pd(II). On the other hand in

Table 3

$$\text{Ar-Cl} + \text{R-CH=CH}_2 \xrightarrow{\text{Pd-MPTA-1, Cs}_2\text{CO}_3, \text{H}_2\text{O, Reflux}} \text{Ar-CH=CH-R}$$

Pd-MPTA catalyzed C–C cross-coupling of aryl chlorides<sup>a</sup>

Entry	Aromatic chlorides <sup>a</sup>	Aromatic alkenes	Time (h)	Yield (%) <sup>b</sup>	Products	TOF (h <sup>-1</sup> ) <sup>c</sup>
1			14	55		55
2			12	60		70
3			10	62		87
4			12	58		68
5			14	58		59

<sup>a</sup> Reaction conditions: Ar–Cl (1.0 equiv.), alkene (1.5 equiv.), Cs<sub>2</sub>CO<sub>3</sub> (2 equiv.), water (4 ml), 100 °C, catalyst (10 mg).

<sup>b</sup> Isolated yield of pure product.

<sup>c</sup> Turn over frequency (TOF) = moles of substrate converted per mole of Pd per h.

the UV–vis spectrum of Pd–MPTA-1 (Fig. 2) this peak at 400 nm was entirely removed, indicating the reduction of Pd(II) to Pd(0) in Pd–MPTA-1. The new broad absorption band in the wavelength range 310–360 nm is observed in Pd–MPTA-1. This could be attributed to the formation of Pd-nanoparticles capped at the surface of the mesoporous polymer that absorbs light via valence-conduction band transitions and also light scattering due to their nanoscale size [44]. The TEM image of the catalyst is shown in Fig. 3a. From this image it is clear that Pd–MPTA-1 has nanosphere like morphology with particles of dimensions ca. 5.0–10.0 nm and these are distributed uniformly throughout the material. The high-resolution TEM image in the (Fig. 3b) shows crystalline nature of the Pd nanoparticles. The interplanar spacing of the 1D fringes is 0.214 nm (Fig. 3c), which agrees well with the (1 1 1) lattice spacing of face-centered cubic Pd(0) [45]. The TEM image (Fig. 4) of the recovered catalyst after one catalytic cycle revealed that the size of palladium nanoparticles is retained after the catalytic reaction. FE SEM image shown in Fig. 5 further illustrates uniform spherical particle morphology of the Pd–MPTA-1 catalyst. The EDX (energy dispersive X-ray) spectrum (Fig. 6) of the black colored material confirmed the presence of Pd and its loading amount was

marginally higher than that obtained from AAS bulk chemical analysis (0.397 wt% vis-à-vis 0.325 wt%).

### 3.2. Catalysis

Substituted aryl iodides underwent coupling reaction with a variety of olefins in the presence of Pd–MPTA-1 and K<sub>2</sub>CO<sub>3</sub> in water very efficiently. The results are reported in the Table 1. The reaction was consistent irrespective on the nature of substituent groups (electron withdrawing or electron donating) attached with the aromatic ring. A heteroaryl iodide also underwent this reaction with similar efficiency (Table 1, entry 12). *meta*-substituted aryl iodide couples with styrene (Table 1, entry 13) without any difficulty. Fluoro group present in the aromatic ring of aryl iodide (Table 1, entry 13) remains inert during the course of reaction. Several sensitive functional groups such as –OCH<sub>3</sub>, –CH<sub>3</sub>, –CN, –CHO, –NO<sub>2</sub> attached with the aromatic ring are compatible for this procedure leading to the formation of coupling products [46] that can be manipulated in the synthesis of important molecules. Bromobenzenes with different functionalities underwent coupling reaction very efficiently in presence of Cs<sub>2</sub>CO<sub>3</sub> base (Table 2). The turn over

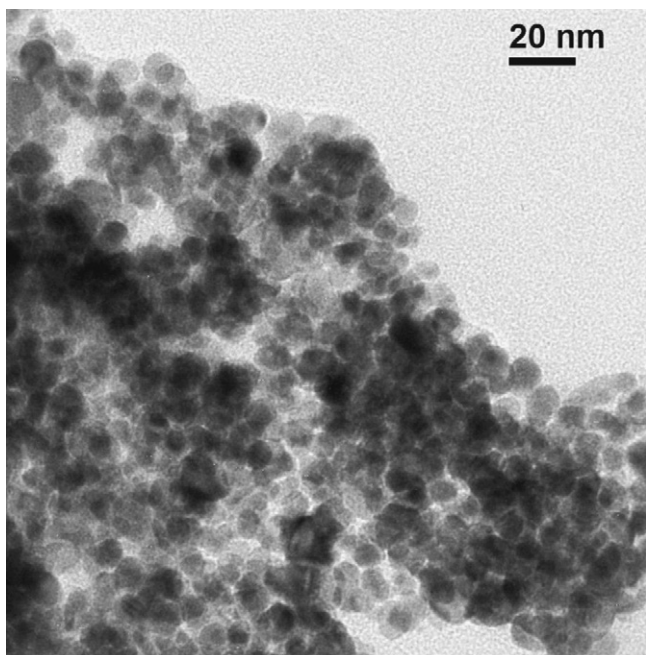


Fig. 4. TEM image of the recovered catalyst after one catalytic cycle.

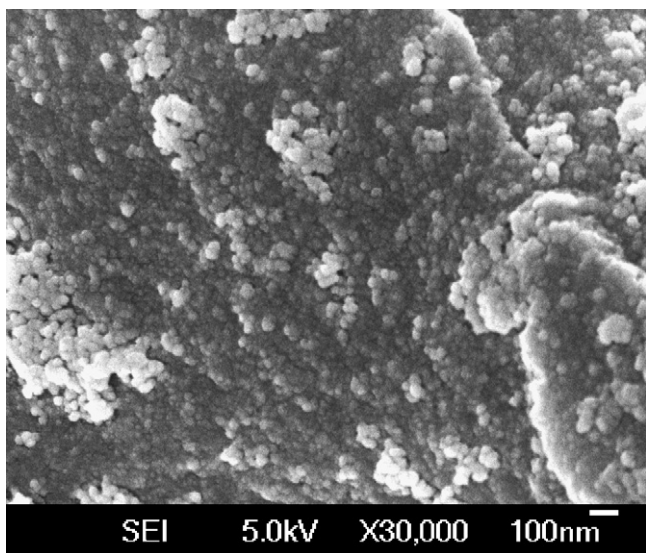


Fig. 5. FE SEM image of the catalyst Pd-MPTA-1.

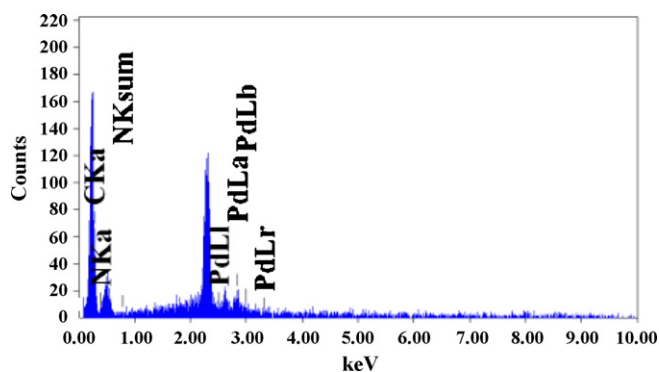


Fig. 6. EDX spectrum of the Pd-MPTA-1 catalyst.

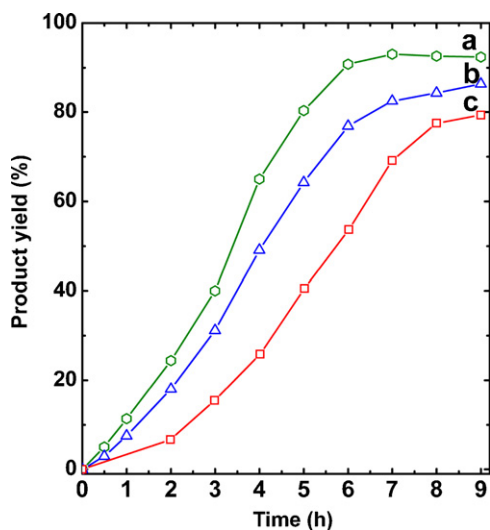
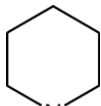
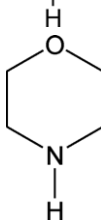
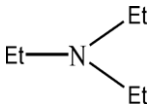

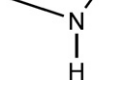


Fig. 7. Conversion as a function of reaction time for the Pd-MPTA-1 catalyzed Heck reaction between iodobenzene and styrene: first (a), second (b) and third cycles (c).

frequencies (TOFs) for different reactions are also quite high, suggesting the catalytic efficiency of Pd tethered mesoporous organic polymer. A heteroaryl bromide (Table 2, entry 5) is compatible for this coupling too. Substituted chlorobenzenes underwent this coupling reaction (Table 3) and gave the coupling products with low TOFs. They took long reaction times and gave the coupling products in low yield compared to that of substituted iodobenzenes and bromobenzenes. However, catalytic activity of our Pd-MPTA-1 is considerably higher than the other heterogeneous Pd-catalysts used in the Heck coupling of aryl chlorides [47]. This result follows the general trend of the catalytic activity in the decreasing order: iodobenzenes > bromobenzenes > chlorobenzenes.

Table 4

Heck coupling over Pd-MPTA-1 in water using different bases.

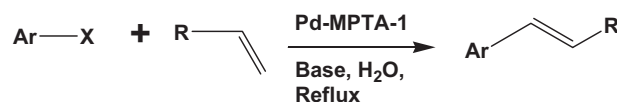
Bases used	Yield (%)
Na <sub>2</sub> CO <sub>3</sub>	80
K <sub>2</sub> CO <sub>3</sub>	92
	
	33
	40
	65
	35

**Table 5**  
Heck coupling over Pd–MPTA-1 using different solvents.

Solvent	Temperature (°C)	Yield (%)
THF	66	40
Toluene	110	15
Acetonitrile	82	25
DMF	110	70
Dichloromethane	40	10

In order to optimize the reaction conditions for a particular base the coupling reaction of iodobenzene and styrene was carried out in water by using different bases and the results are given in Table 4. As seen in this table that inorganic bases showed maximum conversion over the organic bases. This could be attributed to greater solubility of the inorganic bases in water. The reaction becomes very fast when  $K_2CO_3$  was used as a base. Although the coupling reaction of iodobenzene and styrene proceeds in the conventional organic solvents such as DMF,  $CH_3CN$  (Table 5) but the best result was obtained when water was used as the solvent. It may be partly due to the fact that  $K_2CO_3$  have greater solubility in water and thus showing stronger basicity than in organic solvents [48].

The catalytic activity of Pd anchored mesoporous polymer is studied both at high temperature (373 K) as well as at room temperature (298 K). As seen from the table, catalyst is highly reactive at high temperature and it takes only 4–7 h for the completion of coupling reactions, whereas at room temperature no conversion of product of coupling reaction is observed (Table 1, entry 2). The coupling reaction between iodobenzene and styrene has been taken as a representative case to check the recycling efficiency of the palladium anchored catalyst. The Pd loading in the fresh catalyst was estimated by AAS analysis. Pd loading in the fresh catalyst was 0.325%. We have plotted the progress of the reaction as the function of time for three consecutive catalytic cycles for the coupling reaction of iodobenzene and styrene in Fig. 7 over Pd–MPTA-1 catalyst. Pd content of the catalyst has been reduced marginally at this stage (Pd loading 0.314%). As seen from the figure that Pd–MPTA-1 catalyst can be efficiently recycled and reused for three repeating cycles without appreciable decrease in product yield.



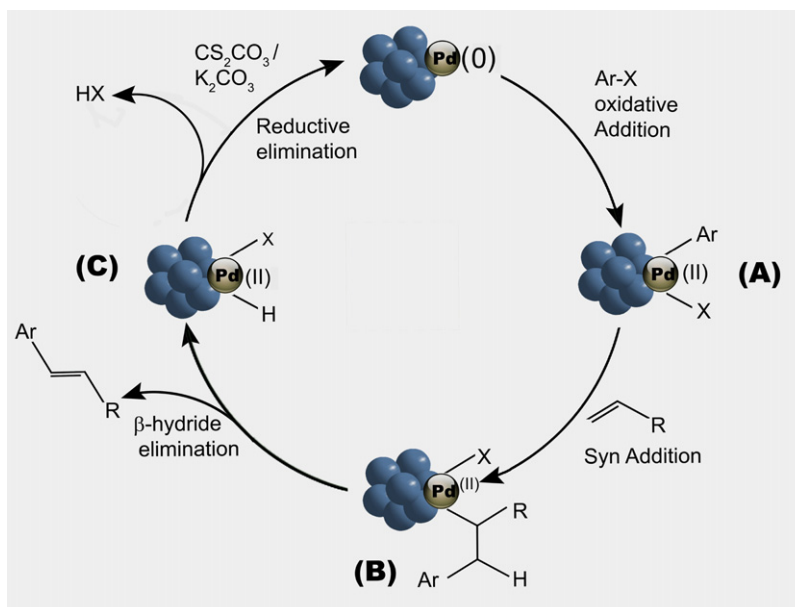
Ar= Aryl, Heteroaryl

R= Phenyl,  $-CO_2Et$ ,  $-CO_2nBu$ ,  $-CO_2H$

X= I, Br, Cl

**Scheme 1.** Cross coupling of aryl halides and olefins over Pd-containing mesoporous polymer.

Plausible reaction pathway for Heck coupling reaction over Pd–MPTA-1 is shown in Fig. 8. Here the palladium nanoparticles present at the surface of Pd–MPTA-1 facilitates the oxidative addition with aryl halide to generate complex (A). Alkene, which inserts itself into the palladium–carbon bond in a syn-addition fashion gives complex (B) [49,50]. Complex (B) follows beta-hydride elimination step to produce alkene with the formation of another palladium complex (C). Pd(0) species could be regenerated by reductive elimination of (C) by  $Cs_2CO_3$  or  $K_2CO_3$  in the final step [51]. AAS elemental analysis of the filtrate of the reaction mixture indicates no detectable amount of palladium leached out during the catalytic reaction. Hot filtration technique was used for the establishment of the fact further. In this technique, a mixture of iodobenzene (204 mg, 1 mmol), styrene (156 mg, 1.5 mmol), Pd–MPTA-1 (10 mg) and  $K_2CO_3$  (276 mg, 2 mmol) in 4 ml of water was kept into reflux at  $100^\circ C$  for 4 h. At this stage yield of the product was 67.2%. The catalyst was filtered off under hot condition and with the filtrate the reaction was continued at the same temperature and for another 4 h in presence of base. No increase in yield of product compared to the yield that was obtained after 4 h was observed (67.2 and 67.0%, before and after hot filtration test, respectively as determined by  $^1H$  NMR). This result suggests that almost no leaching of palladium occurred during the course of reaction (at this stage any leached Pd into the reaction would have enhanced the conversion to a considerable extent otherwise) and thus our Pd–MPTA-1 catalyzed Heck coupling reaction using water as reaction medium is purely heterogeneous in nature (Scheme 1).



**Fig. 8.** Proposed mechanistic pathway for Heck coupling over Pd–MPTA-1.



## 4. Conclusion

In summary we have developed an environment-friendly catalytic system based on functionalized mesoporous polymer material grafted with Pd nanoparticle at its surface. Heck C–C coupling reaction for a variety of aryl and heteroaryl iodides, bromides and chlorides undergoes very efficiently using this mesoporous polymer supported palladium catalyst in water as reaction medium. The method provides green protocol that water as a solvent/reaction medium prevents environmental concerns. The catalyst can be recycled without loss of efficiency and thus the strategy described herein has high potential in eco-friendly catalysis.

## Acknowledgements

AB wishes to thank DST New Delhi for providing instrumental facilities through the Nano Mission Initiatives. JM and AM thank CSIR, New Delhi for their respective senior research fellowships.

## References

- [1] R.F. Heck Jr., J.P. Nolley, *J. Org. Chem.* 37 (1972) 2320–2322.
- [2] R.F. Heck, *Acc. Chem. Res.* 12 (1979) 146–151.
- [3] A.F. Littke, G.C. Fu, *Angew. Chem. Int. Ed.* 41 (2002) 4176–4211.
- [4] C.F.J. Barnard, *Organometallics* 27 (2008) 5402–5422.
- [5] G.P. McGlacken, L.M. Bateman, *Chem. Soc. Rev.* 38 (2009) 2447–2464.
- [6] H. Kawada, M. Iwamoto, M. Utsugi, M. Miyano, M. Nakada, *Org. Lett.* 6 (2004) 4491–4494.
- [7] G.A. Molander, F. Dehmel, *J. Am. Chem. Soc.* 126 (2004) 10313–10318.
- [8] R. Szabo, M.D. Crozet, P. Vanelle, *Synthesis* 127 (2008) 127–135.
- [9] L.J. Jeffrey, R. Sarpong, *Tetrahedron Lett.* 50 (2009) 1969–1972.
- [10] L.F. Tietze, G. Kettischau, U. Heuschert, G. Nordmann, *Chem. Eur. J.* 7 (2001) 368–373.
- [11] M. Beller, A. Tafesh, W.A. Herrmann, German Patent DE 19503/119 (1996).
- [12] S. Durgadas, V.K. Chatare, K. Mukkanti, S. Pal, *Appl. Organomet. Chem.* 24 (2010) 680–684.
- [13] G.T. Crisp, *Chem. Soc. Rev.* 27 (1998) 427–436.
- [14] F. Diederich, P.J. Stang (Eds.), *Metal-Catalyzed Cross-Coupling Reactions*, Wiley, New York, 1998.
- [15] D. Astruc, F. Lu, J.R. Aranzas, *Angew. Chem. Int. Ed.* 44 (2005) 7852–7872.
- [16] N.T.S. Phan, M. Van Der Sluys, C.W. Jones, *Adv. Synth. Catal.* 348 (2006) 609–679.
- [17] G.J. Hutchings, *J. Mater. Chem.* 19 (2009) 1222–1235.
- [18] Y. Kume, K. Qiao, D. Tomida, C. Yokoyama, *Catal. Commun.* 9 (2008) 369–375.
- [19] F. Lang, H.R.A. May, B.L. Iversen, B.D. Chandler, *J. Am. Chem. Soc.* 125 (2003) 14832–14836.
- [20] K. Sarkar, M. Nandi, M. Islam, T. Mubarak, A. Bhaumik, *Appl. Catal. A: Gen.* 352 (2009) 81–86.
- [21] R. Bernini, S. Cacchi, G. Fabrizi, G. Forte, F. Petrucci, A. Prastaro, S. Niembro, A. Shafir, A. Vallribera, *Green Chem.* 12 (2010) 150–158.
- [22] S. Ungureanu, H. Deleuze, O. Babot, M.F. Achard, C. Sanchez, M.I. Popa, R. Backov, *Appl. Catal. A: Gen.* 390 (2010) 51–58.
- [23] L.M. Neal, H.E. Hagelin-Weaver, *J. Mol. Catal. A: Chem.* 284 (2008) 141–148.
- [24] K.E. Price, D.T. McQuade, *Chem. Commun.* (2005) 1714–1716.
- [25] D.D. Das, A. Sayari, *J. Catal.* 246 (2007) 60–65.
- [26] J. Demel, S.E. Sujandi, J. Park, P. Cejka, Stepnicka, *J. Mol. Catal. A: Chem.* 302 (2009) 28–35.
- [27] S.L. Jain, B.S. Rana, B. Singh, A.K. Sinha, A. Bhaumik, M. Nandi, B. Sain, *Green Chem.* 12 (2010) 374–377.
- [28] A. Modak, J. Mondal, V.K. Aswal, A. Bhaumik, *J. Mater. Chem.* 20 (2010) 8099–8106.
- [29] K.M. Parida, D. Rath, S.S. Dash, *J. Mol. Catal. A: Chem.* 318 (2010) 85–93.
- [30] Y. Meng, D. Gu, F. Zhang, Y.F. Shi, L. Cheng, D. Feng, Z.X. Wu, Z.X. Chen, Y. Wan, A. Stein, D. Zhao, *Chem. Mater.* 18 (2006) 4447–4464.
- [31] D. Chandra, B.K. Jena, C.R. Raj, A. Bhaumik, *Chem. Mater.* 19 (2007) 6290–6296.
- [32] M. Nandi, R. Gangopadhyay, A. Bhaumik, *Micropor. Mesopor. Mater.* 109 (2008) 239–247.
- [33] J. Schuster, R. Koehn, A. Keilbach, M. Doeblinger, H. Amenitsch, T. Bein, *Chem. Mater.* 21 (2009) 5754–5762.
- [34] Y.L. Zhang, S. Wei, F.J. Liu, Y.C. Du, S. Liu, Y.Y. Ji, T. Yokoi, T. Tatsumi, F.S. Xiao, *Nano Today* 4 (2009) 135–142.
- [35] J.K. Cho, R. Najman, T.W. Dean, O. Ichihara, C. Muller, M. Bradley, *J. Am. Chem. Soc.* 128 (2006) 6276–6277.
- [36] B. Karimi, D. Enders, *Org. Lett.* 8 (2006) 1237–1240.
- [37] H. Zhao, G.M. Zheng, W.Y. Hao, M.Z. Cai, *Appl. Organomet. Chem.* 24 (2010) 92–98.
- [38] S.A. Patel, K.N. Patel, S. Sinha, B.V. Kamath, *J. Mol. Catal. A: Chem.* 332 (2010) 70–75.
- [39] J. Dupont, R.F. de Souza, P.A.Z. Suarez, *Chem. Rev.* 102 (2002) 3667–3691.
- [40] O. Metin, F. Durap, M. Aydemir, S. Ozkar, *J. Mol. Catal. A: Chem.* 337 (2011) 39–44.
- [41] N. Azizi, F. Aryanasab, L. Torkiyan, A. Ziyaei, M.R. Saidi, *J. Org. Chem.* 71 (2006) 3634–3635.
- [42] M. Lamblin, L. Nassar-Hardy, J.C. Hierro, E. Fouquet, F.X. Felpin, *Adv. Synth. Catal.* 352 (2010) 33–79.
- [43] D. Chandra, A. Bhaumik, *J. Mater. Chem.* 19 (2009) 1901–1907.
- [44] A.V. Gaikwad, G. Rothenberg, *Phys. Chem. Chem. Phys.* 8 (2006) 3669–3675.
- [45] Q. Liu, J.C. Bauer, R.E. Schaak, J.H. Lunsford, *Angew. Chem. Int. Ed.* 47 (2008) 6221–6224.
- [46] <sup>1</sup>H and <sup>13</sup>C NMR chemical shifts for different coupling products reported in Tables 1, 2 and 3;
  - trans-stilbene (table\* 1, entry 1):** White solid; <sup>1</sup>H NMR (300 MHz, CDCl<sub>3</sub>) δ 7.44 (4H, d, J=6 Hz), 7.30 (5H, t), 7.19 (3H, t); <sup>13</sup>C NMR (300 MHz, CDCl<sub>3</sub>) δ 137.4, 128.8, 128.2, 127.7, 126.6;
  - trans-cinnamic acid (table\* 1, entry 3):** White solid; <sup>1</sup>H NMR (500 MHz, CDCl<sub>3</sub>) δ 7.74 (1H, d, J=20 Hz), 7.49 (2H, d, J=2 Hz), 7.42–7.22 (3H, m), 6.36 (1H, d, J=20 Hz); <sup>13</sup>C NMR (500 MHz, CDCl<sub>3</sub>) δ 172.4, 147.2, 134.2, 130.8, 129.3, 128.0, 117.4;
  - trans-4-methoxycinnamic acid (table\* 1, entry 4):** White solid; <sup>1</sup>H NMR (300 MHz, CDCl<sub>3</sub>) δ 7.70 (1H, d, J=18 Hz), 7.45 (2H, d, J=9 Hz), 6.86 (2H, d, J=9 Hz), 6.27 (1H, d, J=15 Hz), 3.77 (3H, s); <sup>13</sup>C NMR (300 MHz, CDCl<sub>3</sub>) δ 171.9, 161.8, 146.7, 130.1, 126.9, 114.6, 55.5;
  - n-Butyl trans-cinnamate; 1; (table\* 1, entry 5):** Colorless oily liquid; <sup>1</sup>H NMR (300 MHz, CDCl<sub>3</sub>) δ 7.63 (1H, d, J=15 Hz), 7.46 (2H, d, J=9.3 Hz), 7.30–7.22 (3H, m), 6.39 (1H, d, J=18 Hz), 4.15 (2H, t), 1.66–1.59 (2H, m), 1.37–1.30 (2H, m), 0.91 (3H, t); <sup>13</sup>C NMR (300 MHz, CDCl<sub>3</sub>) δ 167.2, 144.7, 134.5, 129.2, 128.3, 127.9, 118.3, 64.5, 30.8, 19.3, 13.8;
  - n-Butyl trans-4-methyl cinnamate (table\* 1, entry 6):** Pale yellow liquid, <sup>1</sup>H NMR (300 MHz, CDCl<sub>3</sub>) δ 7.69 (1H, d, J=18 Hz), 7.43 (2H, d, J=12 Hz), 7.26 (2H, d, J=18 Hz), 6.42 (2H, d, J=15 MHz), 4.23 (2H, t), 2.39 (3H, s), 1.71–1.64 (2H, m), 1.48–1.38 (2H, m), 0.995 (3H, t);
  - trans-4-nitrocinnamic acid; 1; (table\* 1, entry 7):** White solid, <sup>1</sup>H NMR (300 MHz, DMSO-d<sub>6</sub>) δ 8.25 (2H, d, J=9 Hz), 7.99 (2H, d, J=9 Hz), 7.71 (1H, d, J=15 Hz), 6.76 (1H, d, J=15 Hz); <sup>13</sup>C NMR (300 MHz, DMSO-d<sub>6</sub>) δ 167.5, 148.5, 141.8, 141.3, 129.8, 124.4, 124.2;
  - trans-4-methoxystilbene (table\* 1, entry 8):** White solid, <sup>1</sup>H NMR (500 MHz, CDCl<sub>3</sub>) δ 7.09 (1H, d, J=9 Hz), 7.001 (1H, d, J=9.6 Hz), 6.919 (2H, d, J=8.5 Hz), 7.508 (2H, d, J=9 Hz), 7.473 (2H, d, J=8.5 Hz), 7.368 (2H, t), 7.260 (1H, t), 3.838 (3H, s); <sup>13</sup>C NMR (500 MHz, CDCl<sub>3</sub>) δ 159.4, 137.7, 130.3, 128.7, 128.3, 127.8, 127.3, 126.7, 126.3, 114.2, 55.4;
  - trans-4-methylstilbene (table\* 1, entry 9):** <sup>1</sup>H NMR (300 MHz, CDCl<sub>3</sub>) δ 7.43 (2H, d, J=7.2 Hz), 7.34 (2H, d, J=6 Hz), 7.10 (2H, d, J=9 Hz), 7.32 (3H, t), 7.18 (2H, d, J=6 Hz), 2.28 (3H, t);
  - trans-4-nitrostilbene (table\* 1, entry 10):** Pale yellow solid, <sup>1</sup>H NMR (300 MHz, CDCl<sub>3</sub>) δ 8.23 (2H, d, J=6 Hz), 7.65 (2H, d, J=9 Hz), 7.56 (2H, d, J=6 Hz), 7.42–7.33 (4H, m), 7.17 (1H, d, J=18 Hz); <sup>13</sup>C NMR (300 MHz, CDCl<sub>3</sub>) δ 146.8, 143.9, 133.2, 133.4, 128.9, 128.9, 127.1, 126.9, 126.3, 124.2;
  - trans-4-methylcinnamic acid (table\* 1, entry 11):** White solid, <sup>1</sup>H NMR (300 MHz, CDCl<sub>3</sub>) δ 7.79 (1H, d, J=20 Hz), 7.46 (2H, d, J=10 Hz), 7.26 (2H, d, J=20 Hz), 6.42 (1H, d, J=15 Hz), 2.98 (3H, s); <sup>13</sup>C NMR (300 MHz, CDCl<sub>3</sub>) δ 172.5, 147.2, 141.4, 131.5, 129.8, 128.5, 116.3, 21.6;
  - 3-pyridyl styrene (table\* 1, entry 12):** Brown colored solid, <sup>1</sup>H NMR (300 MHz, CDCl<sub>3</sub>) δ 8.69 (1H, s), 8.46 (1H, d, J=3 Hz), 7.78 (1H, d, J=9 Hz), 7.50 (2H, d, J=6 Hz), 7.37 (2H, t), 7.29–7.21 (2H, m), 7.15 (1H, d, J=18 Hz), 7.04 (1H, d, J=18 Hz); <sup>13</sup>C NMR (300 MHz, CDCl<sub>3</sub>) δ 148.4, 136.5, 132.9, 132.6, 130.8, 128.7, 128.1, 126.6, 124.7, 123.5;
  - trans-3-fluorostilbene (table\* 1, entry 13):** Brownish white solid, <sup>1</sup>H NMR (300 MHz, CDCl<sub>3</sub>) δ 7.55 (2H, d, J=9 Hz), 7.41–7.30 (7H, m), 7.11 (1H, d, J=6 Hz), 6.97 (1H, s); <sup>13</sup>C NMR (300 MHz, CDCl<sub>3</sub>) δ 161.7, 139.9, 136.9, 130.4, 128.8, 128.1, 127.6, 126.8, 126.6, 114.6, 113.0;
  - trans-4-formylstilbene (table\* 2, entry 4):** White solid, <sup>1</sup>H NMR (300 MHz, DMSO-d<sub>6</sub>) δ 9.96 (1H, s), 7.90 (2H, d, J=9 Hz), 7.81 (2H, d, J=9 Hz), 7.65 (2H, d, J=9 Hz), 7.49–7.31 (5H, m); <sup>13</sup>C NMR (300 MHz, DMSO-d<sub>6</sub>) δ 192.3, 143.0, 136.4, 135.0, 131.9, 129.9, 128.7, 128.3, 127.2, 126.9, 126.9;
  - trans-4-cyanostilbene (table\* 2, entry 3):** Grey solid, <sup>1</sup>H NMR (300 MHz, CDCl<sub>3</sub>) δ 7.18 (1H, d, J=12 Hz), 7.25 (1H, d, J=3 Hz), 7.40–7.31 (2H, m), 7.81 (1H, t), 7.69–7.51 (6H, m); <sup>13</sup>C NMR (300 MHz, CDCl<sub>3</sub>) δ 141.9, 136.4, 132.6, 132.0, 129.0, 128.7, 126.9, 126.8, 119.1, 110.6;
  - 2-thiophenyl ethylacrylate (table\* 2, entry 5):** Brown colored liquid, <sup>1</sup>H NMR (300 MHz, CDCl<sub>3</sub>) δ 7.21 (2H, d, J=6 Hz), 7.04 (1H, t), 6.90 (1H, d, J=18 Hz), 6.66 (1H, d, J=9 Hz), 3.75 (2H, q), 1.25 (3H, t); <sup>13</sup>C NMR (300 MHz, CDCl<sub>3</sub>) δ 167.2, 144.7, 134.5, 130.3, 129.2, 128.1, 127.9, 64.5, 13.8.
- [47] S. Mukhopadhyay, G. Rothenberg, A. Joshi, M. Baidossi, Y. Sasson, *Adv. Synth. Catal.* 344 (2002) 348–354.
- [48] Z. Zhang, Z. Zha, C. Gan, C. Pan, Y. Zhou, Z. Wang, M.-M. Zhou, *J. Org. Chem.* 71 (2006) 4339–4342.
- [49] C. Amatore, A. Jutand, *Acc. Chem. Res.* 33 (2000) 314–321.
- [50] J.A. Fritz, J.P. Wolfe, *Tetrahedron* 64 (2008) 6838–6852.
- [51] J.G. de Vries, *Dalton Trans.* (2006) 421–429.